INFORMATION NOT TO BE
RELEASED OUTSIDE NASA
UNTIL PAPER PRESENTED

LABORATORY SIMULATION OF LUNAR SURFACE EROSION BY ROCKETS

By Norman S. Land and D. William Conner

NASA Langley Research Center
Langley Station, Hampton, Va.

Presented at the 13th Annual Institute of Environmental
Sciences Technical Meeting

GPO PRICE $ _____

CFSTI PRICE(S) $ _____

Hard copy (HC) 3.00

Microfiche (MF) .65

ff 653 July 65

Washington, D.C.
April 10-12, 1967

FACILITY FORM 602

N 68-27286 (ACCESSION NUMBER) (THRU) 1

12 (PAGES) (CODE)

TMX-59863 (NASA CR OR TMX OR AD NUMBER) 30 (CATEGORY)

LABORATORY SIMULATION OF LUNAR SURFACE EROSION BY ROCKETS

By: Norman S. Land and D. William Conner
NASA Langley Research Center

Norman S. Land D. William Conner

Mr. Land is an Aerospace Engineer at the NASA Langley Research Center where he has been employed since 1938. He received a BS in AeE, BS in ME from Wayne State University and a MS from the University of Michigan. He has performed research work in hydrodynamics, vibration and flutter, and present field. He is presently assigned to the Environmental Systems Section, Dynamic Loads Division.

Mr. Conner has been employed at the NASA Langley Research Center since 1942 after graduating with a BSME from Ohio Northern University. His early research work was in the field of aerodynamics and covered a broad range of problem areas. He later was placed in charge of the Transonic Dynamics Wind Tunnel. In 1962, he was named to head the new Dynamics Research Laboratory used for space environment research. He is also assistant head of the Structural Dynamics Branch.

Soft landings on the moon or on other planetary bodies having little or no atmosphere can be accomplished only by firing retro-rockets almost to touchdown to counteract the local gravitational acceleration. Both the unmanned Surveyor and the forthcoming manned Apollo Lunar Module use this system. The height at which thrust is terminated must be carefully selected to provide as gentle a landing as possible without incurring problems associated with operating a rocket engine too close to the surface. Erosion of the lunar surface by the engine blast can introduce several hazards which are illustrated in figure 1. These include impairment of visibility at a crucial moment due to outthrown surface material, possible damage to the vehicle by dust particle impact and formation of a crater uneven enough to impair landing stability. Analytical treatment of the problems associated with jet erosion of the lunar surface was initiated by Roberts (refs. 1 and 2) and extended by Hutton of TRW (ref. 3). Such analysis requires companion experimental studies which must be carefully formulated if the results are to be meaningful. Initial experimental effort was reported by Land and Clark in reference 4. This paper describes an experimental technique developed at the NASA Langley Research Center. It includes a brief description of the physical characteristics of the jet impinging a surface, scaling factors considered in devising experiments, experimental apparatus employed and some typical results.

The flow field which causes the erosion of soil by an impinging jet is described in figure 2. Where the surrounding atmosphere is essentially nonexistent, the exhaust will plume-out to extreme angles. The extent of the pluming is dependent upon the exhaust Mach number, the ratio of combustion chamber pressure to external pressure, and the lip angle of the nozzle. (See ref. 5.) When the jet exhaust contacts a solid surface, a bowl-shaped shock wave is formed and the flow below this shock wave is turned radially outward along the surface. At the extension of the jet centerline a stagnation point exists where the velocity is zero. With increasing radial distance the density of outflowing gas decreases rapidly but the radial velocity increases. As a result, the dynamic pressure (or eroding force) reaches a maximum value at some distance from the stagnation point and then decreases with increasing distance. The dynamic pressure of the radially outward flowing gas across the lunar surface causes shear forces on the particles which comprise the surface. Because the dynamic pressure has a maximum value some distance from the stagnation point, erosion starts in a ring and then progresses both inward and outward. Experimental evidence verifies this behavior.

The flow field described above cannot be exactly duplicated in earth-based laboratories for erosion studies because the ambient pressure on the moon cannot be matched in any present-day vacuum chamber containing an exhausting jet. Fortunately, with a ratio of combustion chamber pressure to ambient pressure much lower than infinity, it is possible to nearly match the energy distribution of that portion of the jet flow field considered to influence lunar soil erosion. A pressure ratio as low as 10^5 is probably acceptable. However, caution should be exercised in going to values much lower since the flow field changes radically as the pressure ratio decreases. There have been several instances where peculiar erosion patterns observed in experimental studies probably resulted from pressure ratios which were too low.

The shearing action of the rocket flow field is resisted by several restraints in the surface material. These include interparticle cohesion, particle interlocking, and particle frictional restraint resulting from gravity. Since the exact nature of the lunar surface material is still somewhat questionable, interparticle effects must be considered as a variable in earth-based experiments. Information obtained from Surveyor I led to the general observation that the lunar surface material was somewhat cohesive. The effects of reduced lunar gravity can be simulated for a few seconds with specially designed drop rigs (ref. 6) although the size of the experiment would necessarily be small. Gravity affects not only the dislodging of the particles but also their trajectories. Indeed, calculations indicate that during a lunar landing a significant amount of the ejecta may actually go into orbit (ref. 7).

The flow fields needed for lunar jet erosion studies on the earth can be sufficiently realistic

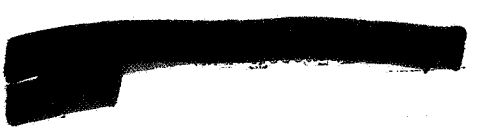

only when obtained in a vacuum environment. Even the largest vacuum chambers and pumping systems do not have capacity to maintain the necessary degree of vacuum when a full-size Lunar Module engine is operated. This limitation, together with economic considerations, introduces the requirement for scaled experiments utilizing small model jets in a large vacuum chamber. Considerable study led to a scaling scheme where the following ratios were matched for both model and full-scale conditions:

$$\frac{\text{kinetic energy of gas at jet exit}}{\text{internal energy of gas at jet exit}} = \gamma(\gamma - 1)M^2 \quad (1)$$

$$\frac{\text{particle friction restraint}}{\text{aerodynamic shear}} = \frac{\sigma g\, Dc \tan \alpha}{C_f \rho V^2} \quad (2)$$

$$\frac{\text{gas density}}{\text{particle density}} = \frac{\rho}{\sigma} \quad (3)$$

where

γ = ratio of specific heats of exhaust gas

M = Mach number

σ = mass density of particle material

g = acceleration due to gravity

D = particle size

c = bed packing factor

$\tan \alpha$ = friction angle of particles

C_f = drag coefficient of exposed particle

ρ = mass density of gas

V = gas velocity

Satisfying the relation of equation (1) insures the proper distribution of kinetic energy in the expansion region outside the nozzle exit (provided the ambient pressure allows adequate jet pluming) and thus helps insure the proper jet flow field. Satisfying the relation of equation (2) insures proper single particle dislodging. In exploratory studies, the best correlation with experimental incipient erosion was obtained when the value of C_f was assumed to be 0.2. Satisfying the relation of equation (3) insures correct momentum interchange between the gas and the particles.

From equations (1), (2), and (3), the length, time, and mass scale relations can be derived.

$$\frac{l_F}{l_M} = \lambda = \frac{\left|\gamma_M - 1\right| R_F \sigma_M \rho_F g_M T_F}{\left|\gamma_F - 1\right| R_M \sigma_F \rho_M g_F T_M} \quad (4)$$

$$\frac{t_F}{t_M} = \lambda \left[\frac{\left|\gamma_F - 1\right| R_M T_M}{\left|\gamma_M - 1\right| R_F T_F}\right] \quad (5)$$

$$\frac{m_F}{m_M} = \lambda^3 \frac{\rho_F}{\rho_M} \quad (6)$$

where

l = length

t = time

λ = length scale factor

m = mass

R = gas constant

T = absolute temperature

Subscripts

F = full scale

M = model

Using these primary relations, the scale relations for other quantities such as velocity and acceleration can be derived. Some factors have been neglected in this scaling system. Probably the most significant factor neglected is that of inter-particle cohesion. As will be illustrated later, the erosion process of fine particles, where cohesive forces predominate, is substantially different from that of larger particles where particle friction is the primary restraint. Thus, if in scaling down particle size, the model particles become small enough to fall within the cohesive range, the model cratering will not truly represent the full-scale conditions.

Experiments were devised consistent with the constraints and scaling relations discussed above. Studies were carried out in chambers having volumes of 108,000 cubic feet and 140,000 cubic feet and a vacuum level of 10^{-4} torr. Various conical and isentropic nozzles have been used with exit diameters ranging from 16 mm to 67 mm, with exit Mach numbers from 2.6 to 5 and with both cold nitrogen and cold helium gases. Various soil simulants have been tried including aluminum oxide, sand, pumice and glass beads ranging in size from about one micron to 10 millimeters.

Early experiments were formulated primarily to investigate the applicability of the erosion relations developed by Roberts in his theoretical study. More recently, experiments scaled specifically for the Lunar Module vehicle have been carried out using the experimental arrangement shown in figure 3 which had the following characteristics:

length scale factor: $\frac{l_F}{l_M} = 19.6$

time scale factor: $\frac{t_F}{t_M} = 10.9$

mass scale factor: $\frac{m_F}{m_M} = 7800$

test gas: helium at 100 torr stagnation pressure and ambient temperature

soil simulants: glass beads (cohesionless soils only)

Use of cold helium with a nozzle contoured to match the LM engine does not provide the proper kinetic energy distribution across the jet exit plane but the correct distribution could be obtained using a nozzle of somewhat different contour. Rather than provide a recontoured nozzle (which requires extensive calculations) nozzle of two shapes providing isentropic flow and conical flow were employed since their respective kinetic energy distributions were believed to bracket the kinetic energy distribution for the full-scale article. Experiments with this configuration simulated full-scale lunar conditions for up to 30 seconds operation of the LM engine eroding material ranging from 2 millimeters to 150 millimeters in size. An adjustable stroking mechanism simulated a range of descent velocities for the last 20 meters above the surface. Primary measurements made in the experiments were crater growth and reduction in visibility.

An X-ray technique, illustrated schematically in figure 4 was used to measure crater growth. The bed of simulated lunar soil was positioned on top of a plate and an X-ray source was located above the soil and just off the axis of the jet. The thickness and material of the plate were sufficient to essentially stop the X-rays except for a slot which extended radially outward from the jet centerline. Below the plate an X-ray cassette containing film was moved across the slot at a constant speed. The film coordinates thus represented radial distance and time. The optical density of the film at any given spot was a measure of the depth of simulated soil above it at the time the spot was exposed. Problems which had to be overcome in using the method included:

1. Providing an X-ray source with constant repeatable output sufficient to penetrate the test depth of 15 centimeters of simulated soil.

2. Obtaining quantitative data over the full range of soil depths from the high contrast film generally used in the X-ray industry.

3. Providing carefully controlled film processing to insure repeatable calibration data.

4. Averaging results to account for uneven film exposure from voids between particles in the larger size soil simulants.

Overall quantitative accuracy in measuring crater depth with this technique was considered to be about ±5 percent of full bed depth.

Impairment to visibility is difficult to measure because of the human factors involved. People react differently to given changes in quantities such as incident lighting, back scatter from dust, or color contrast of the target. Therefore, measurements which are objective rather than subjective provide only rough, qualitative measures of degradation in visibility. Objective measurements were made in these experiments and consisted of the attenuation of beams of light along both horizontal and downwardly inclined (36°) paths from a Lunar Module viewpoint location. The light consisted of a tungsten filament source optically collimated to produce a 0.37 meter (full scale) square beam. Photocells located about seven meters (full scale) from the vehicle centerline sensed the light intensity. In essentially all experiments, light reduction by the ejecta amounted to less than 10 percent with the highest reduction equal to about 20 percent.

The experimental arrangement described above has been used to obtain both general and specific information regarding crater formation. This information includes definition of incipient erosion boundaries and growth of a crater as affected by descent rate, time, and particle size.

Incipient erosion boundary is defined as the height boundary above which a jet of given thrust will not disturb particles on the ground. Figure 5 illustrates a typical boundary. If the particles are relatively large and restrained by particle friction resulting from gravity, there is a boundary as shown on the right side of this figure. As particle size is increased, the jet must come closer to the ground to initiate erosion. If on the other hand the particles are very small, interparticle cohesive force becomes the significant factor. With decrease in particle size, this cohesive force increases and the cohesive cut-off boundary has the shape shown. Theory agrees well with experiment in predicting the incipient erosion boundary for the larger non-cohesive particles but predicts a boundary lower than experiment for the smaller cohesive particles.

Interparticle cohesion significantly affects crater shape as shown in figure 6. For very cohesive particles cratering occurs in an irregular manner with a gouged crater shape with ragged edges and with rays extending radially. This unevenness results because agglomerate masses rather than individual particles erode. For non-cohesive particles, erosion is very regular and the crater shape is symmetrical. To date, attempts to predict erosion behavior of cohesive materials has not been overly successful. Experimental study of cohesive material erosion has been limited mainly because attention has been given to the more critical problem of non-cohesive materials where rate of erosion is greater.

Another difference that has been noted between cohesive and non-cohesive materials occurs at jet cut-off. Craters formed in non-cohesive material are steep sided and slump at jet cut-off into an approximately conical shape. Beds of fine particle cohesive material accumulate subsurface gas pressure which cannot leak off due to the very small pores. When the jet cuts off, this subsurface gas pressure causes an explosive eruption of material. This material would probably strike the spacecraft.

Crater shape and crater growth for a typical non-cohesive material is illustrated in figure 7. For this particular experiment, the jet nozzle

remained stationary as in a hovering condition. The experimentally determined crater profile is shown at four points in time. For this experiment crater measurements did not extend to the jet axis. The deepest portion of the crater occurred at the point of maximum calculated dynamic pressure. Crater depth increased nearly linearly with time with a rather uniform digging rate. Results of experiments covering a range of parameters indicate that for a given jet the digging rate is affected by jet distance from the surface, by type of material, and by material size.

The effect of material size is shown graphically in figure 8 for two experiments scaled for the Lunar Module vehicle. The experiments simulated the vehicle descending at the constant rate of 2.4 feet per second with thrust equal to weight. Thrust was terminated when the legs were about one foot above the surface. The simulated surface was comprised of uniform size particles. For a particle size of 0.08 inch full scale, the crater was insignificant; but for 1.10 inch particles, the crater extended well out toward the vehicle legs. The crater size continued to increase with particle size up to simulated six inch particles which were the largest investigated. Increase in erosion with particle size can be explained through consideration of transfer of momentum from the airstream to the particles. As the particle size increases, the inertia (volume) increases faster than the aerodynamic propelling force (area). Since the larger particles accelerate more slowly than small particles and therefore attain a smaller fraction of the airstream velocity in a given time than do the smaller particles, a greater mass of the larger particles must erode in a given time in order to absorb the excess momentum. For a given nozzle height, as the size of the particles increases, the erosion will increase until, of course, the erosion boundary is reached at which time erosion stops and all airstream momentum is again absorbed in surface shear stress by the static restraining forces.

The lunar conditions in the experiments of figure 8 were certainly overly simplified for simulating the real mission. Rate-of-descent will not necessarily be that slow; jet cut-off may be further above the surface; surface material may well be a mixture of sizes and may even be cohesive. Until the actual mission is carried out and the true soil composition is determined, however, the worst possible set of circumstances must be assumed.

A description has been given of a technique which utilizes models for laboratory simulation of lunar surface erosion by rockets. Various factors involved in this technique have been discussed and some typical results presented. The information provided should prove useful to those who desire to carry out similar investigations.

REFERENCES

1. Roberts, Leonard: The Action of a Hypersonic Jet on a Dust Layer. Paper No. 63-50, Inst. Aerospace Sci., January 1963.

2. Roberts, Leonard: The Interaction of a Rocket Exhaust with the Lunar Surface. Presented at a Specialists Meeting on "The Fluid Dynamic Aspects of Space Flight" (Marseille, France), AGARD, April 20-24, 1964.

3. Hutton, R. E.: An Investigation of Soil Erosion and Its Potential Hazard to LM Lunar Landing. Project Technical Report Task ASPO 22A. TRW Systems, 1966.

4. Land, Norman S., and Clark, Leonard V.: Experimental Investigation of Jet Impingement on Surfaces of Fine Particles in a Vacuum Environment. NASA TN D-2633, 1965.

5. Love, Eugene S., Griegsby, Carl E., Lee, Louise P., and Woodling, Mildred J.: Experimental and Theoretical Studies of Axisymmetric Free Jets. NASA TR R-6, 1959.

6. Carden, Huey D., Herr, Robert W., and Brooks, George W.: Technique for the Simulation of Lunar and Planetary Gravitational Fields Including Pilot Model Studies. NASA TN D-2415, 1964.

7. Cramblit, D. C.: A Consideration of Lunar Surface Ballistics and the Hazards Associated with Spacecraft Landing or Launch Operations. NASA TN D-1526, 1963.

- Reduced visibility
- Vehicle damage by dust particle impact
- Uneven landing surface

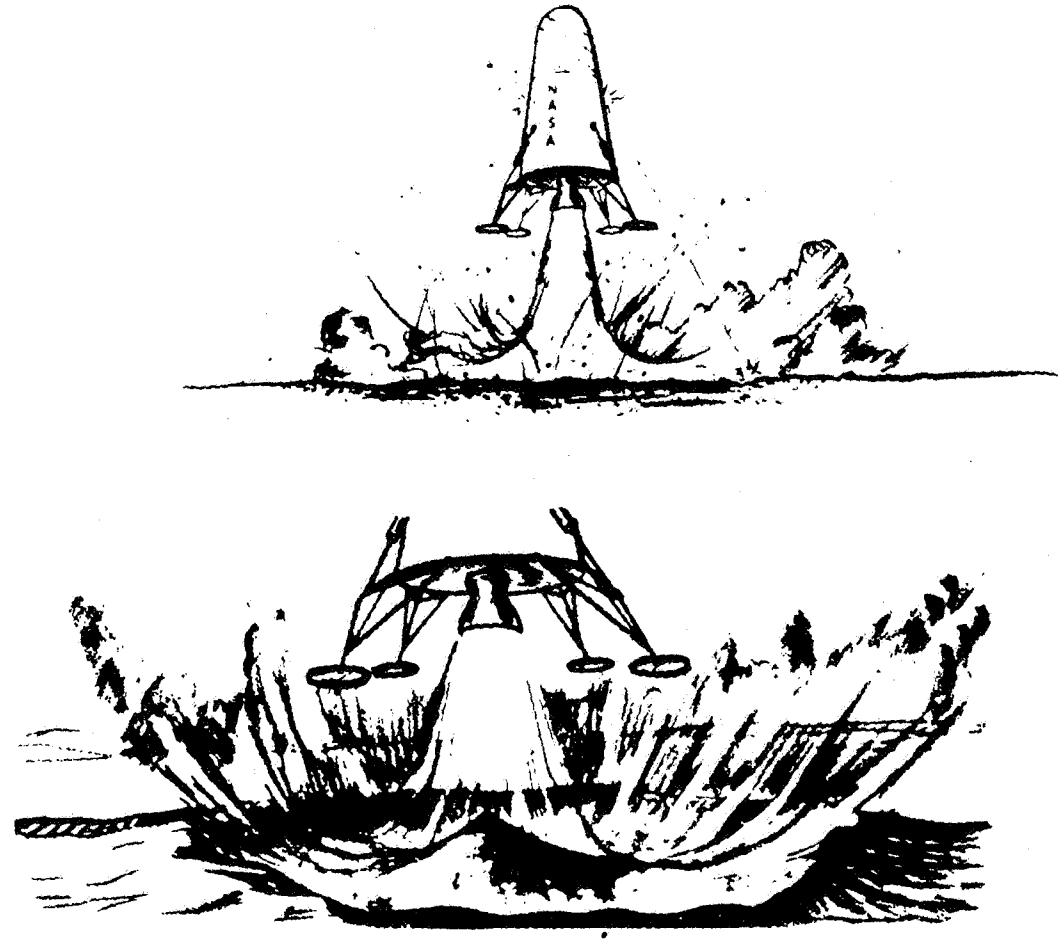

Figure 1.- Lunar landing hazards.

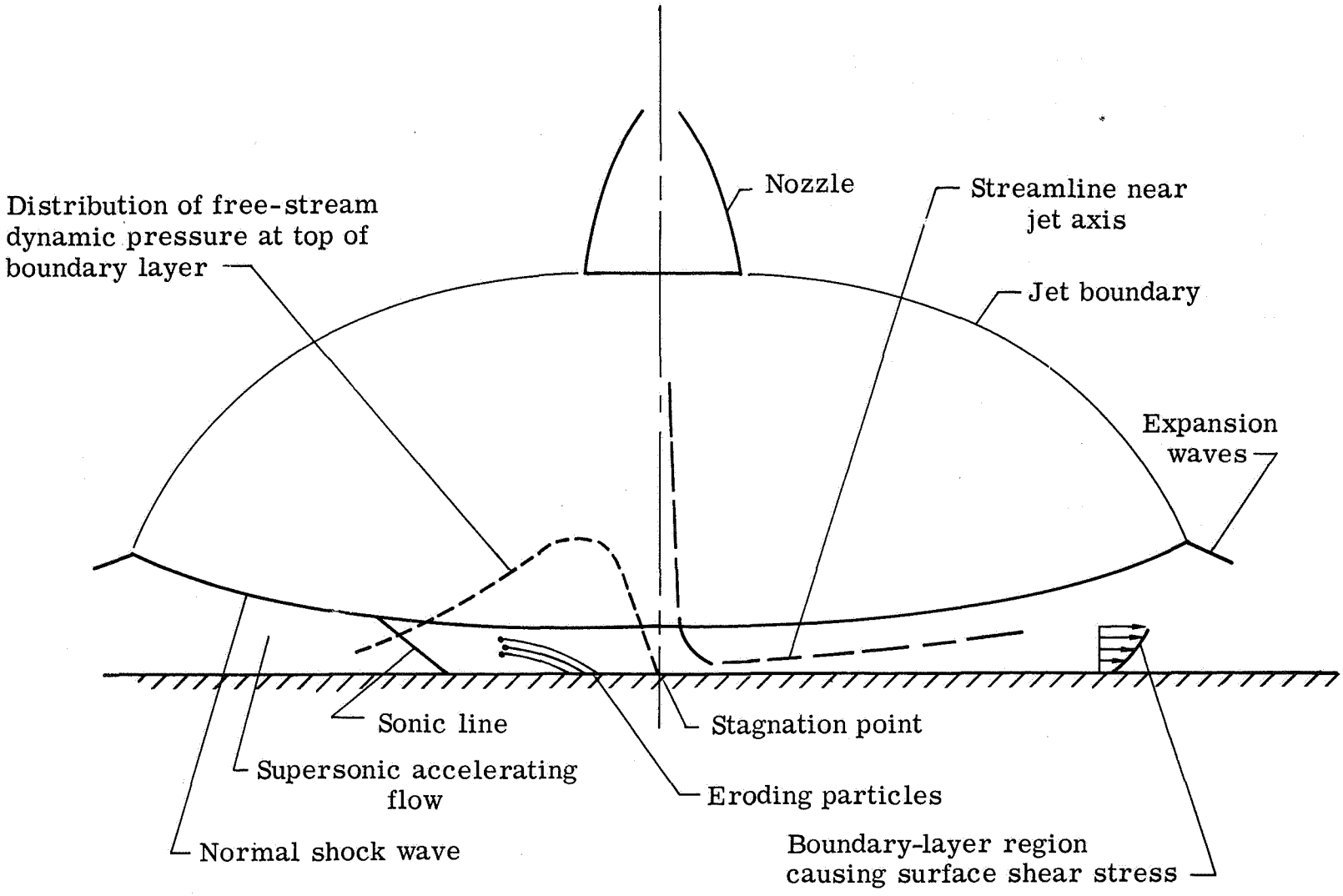

Figure 2.- Plane section of exhaust flow field of jet.

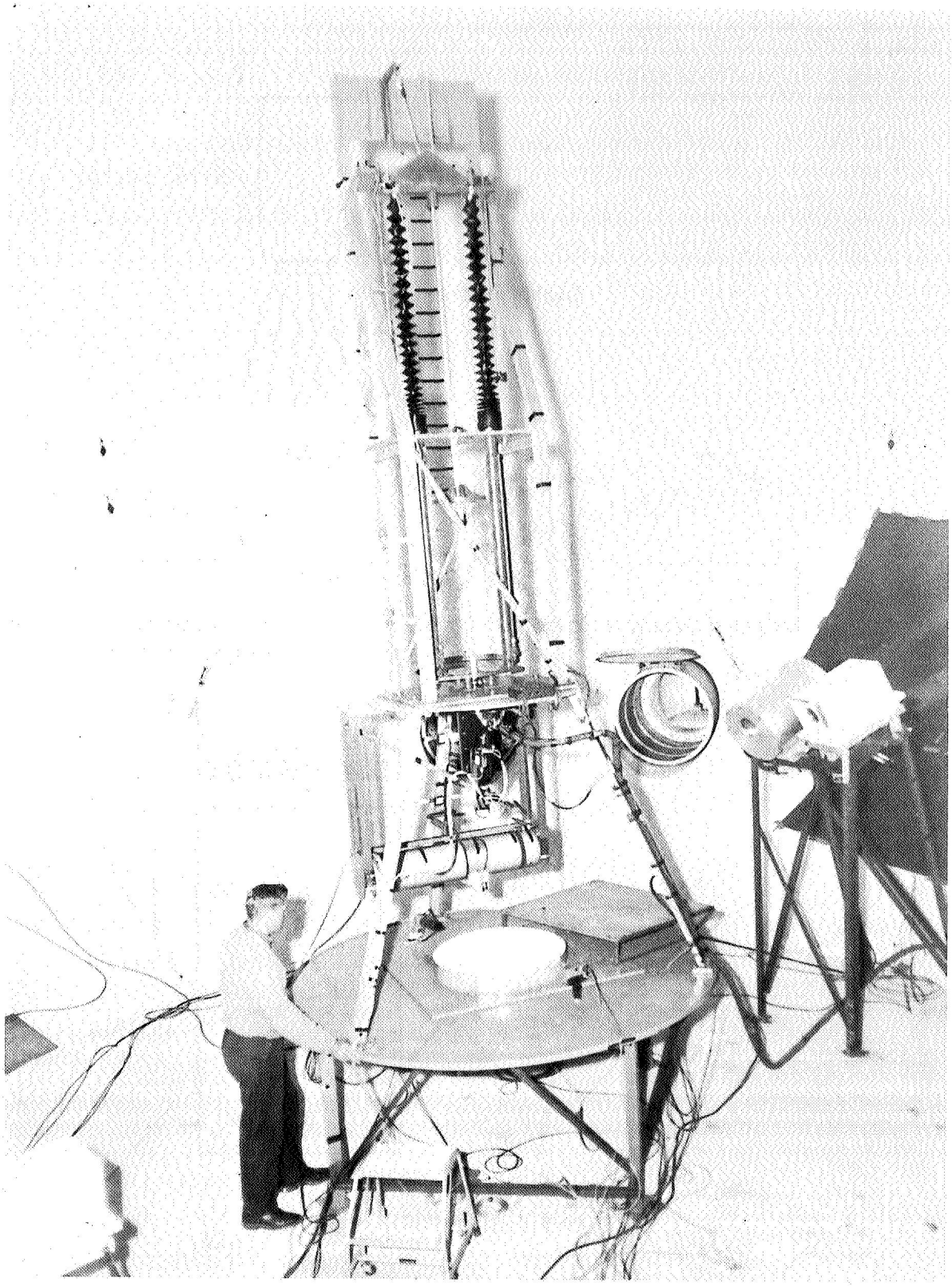

Figure 3.- Experimental apparatus for jet erosion studies.

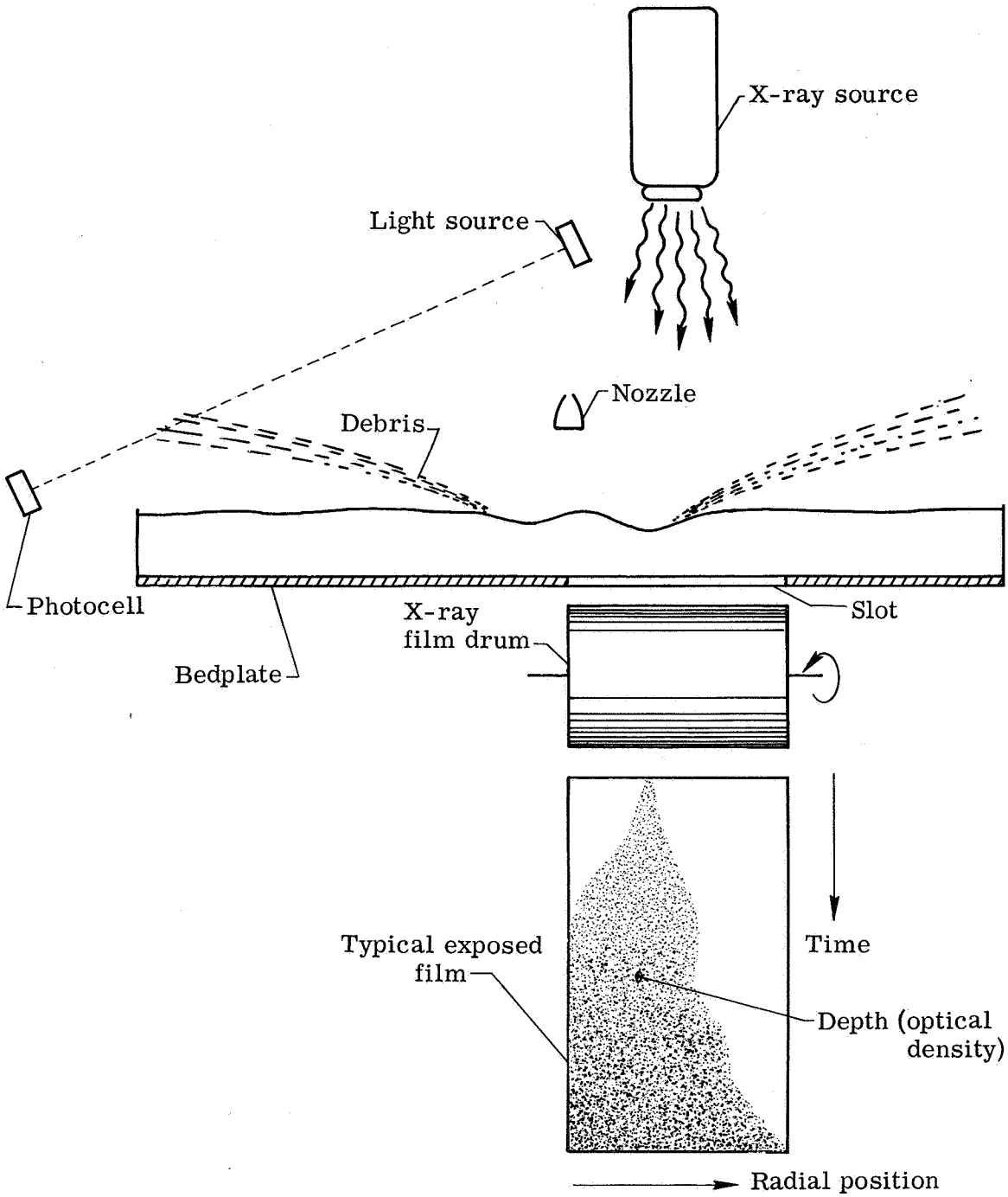

Figure 4.- Schematic of setup.

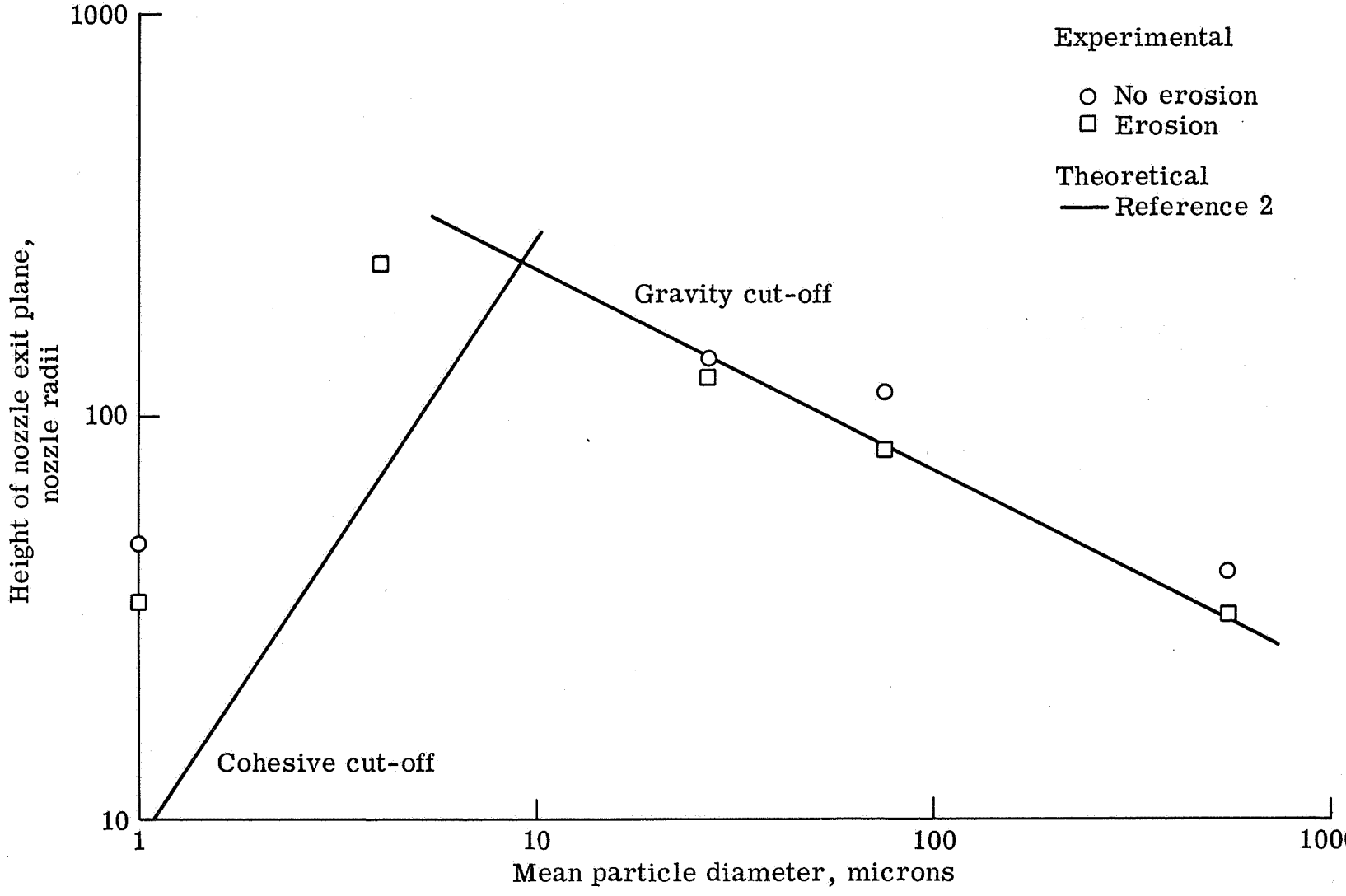

Figure 5.- Typical incipient erosion boundary.

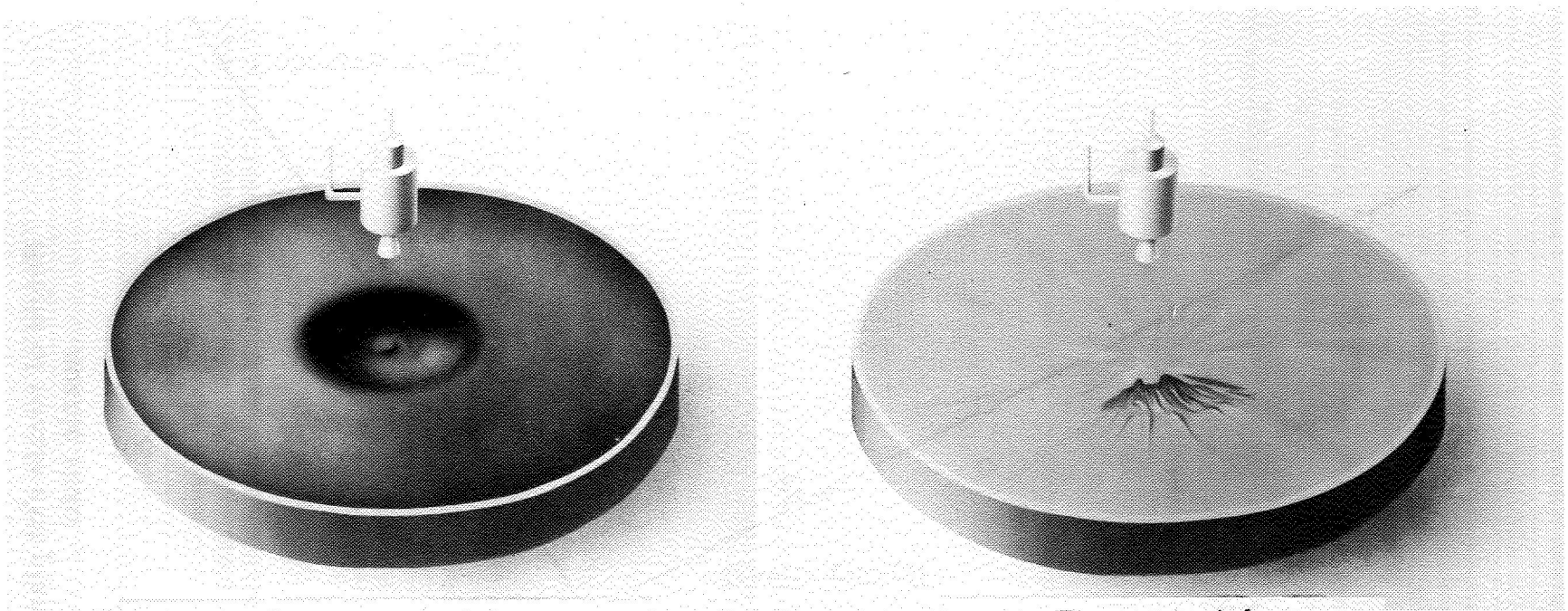

Coarse material
(granules - 600 microns)

Dished crater

Fine material
(dust - 1 micron)

Gouged crater

Figure 6.- Typical craters for cohesive and noncohesive particles.

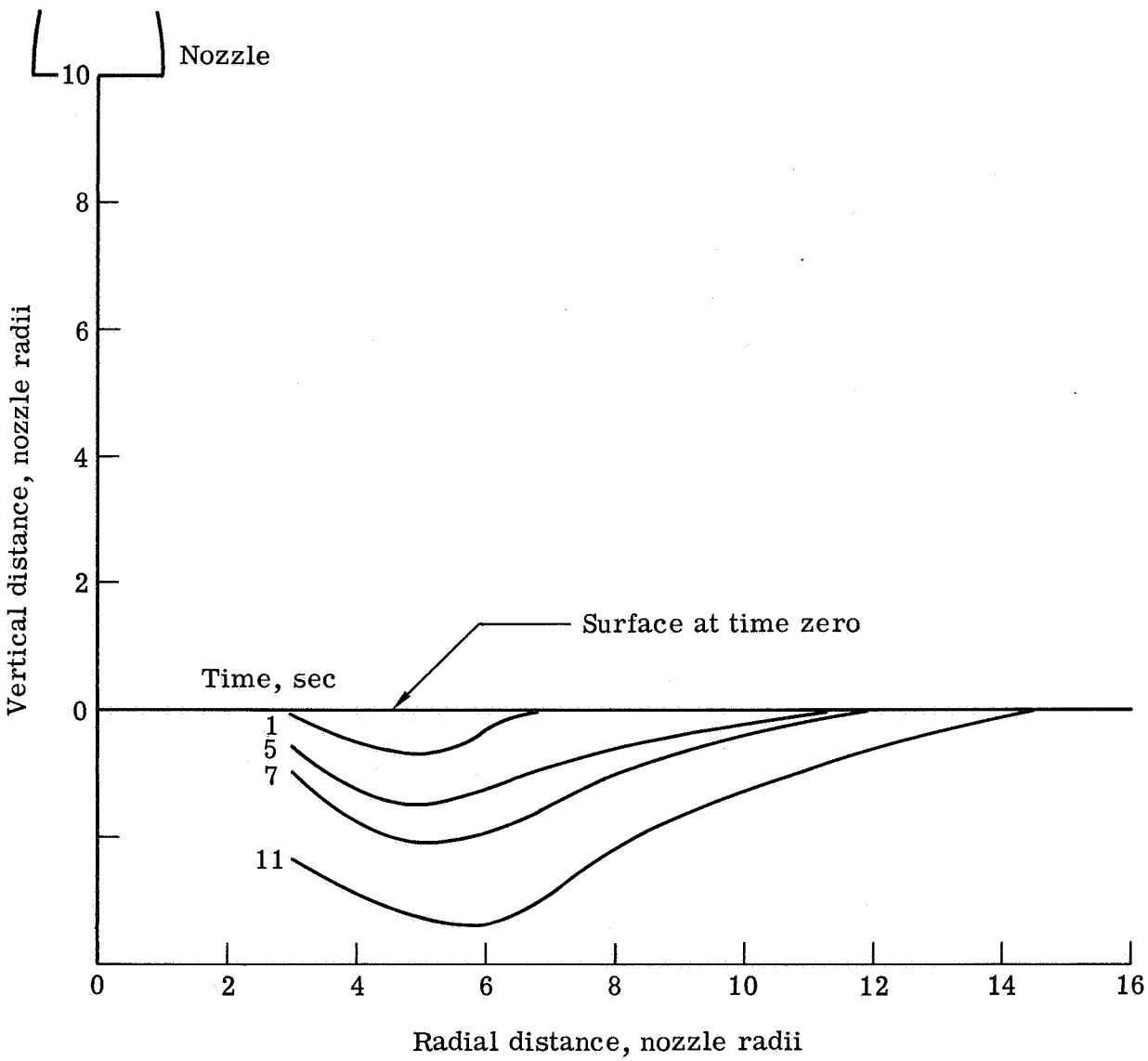

Figure 7.- Typical crater cross-section profile.

Typical results for jet erosion

Descent rate, 2.4 feet/second
Thrust = lm weight under lunar gravity
Thrust terminates 1 ft before touchdown
Crater approximately to scale

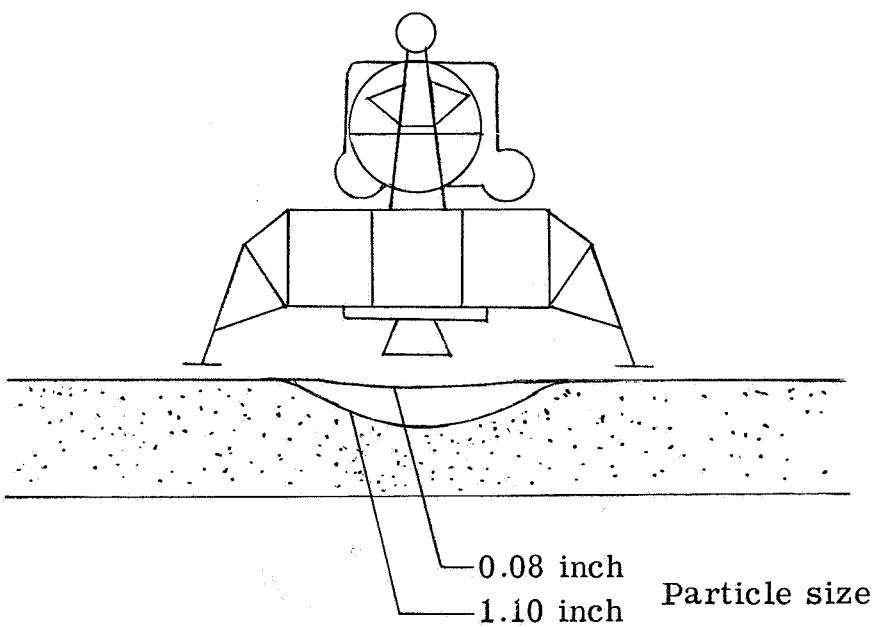

Figure 8.- Effect of particle size on erosion.

NASA-Langley, 1967